Crystallization Kinetics Study on Orthogonal Ordering in *N*-(*p*-*n*-Alkyoxybenzylidene)-*p*-*n*-Alkylanilines (*n*O.*m* Compounds) by Thermal and Electrical Techniques. Part I

Thangaiyan Chitravel[a], Mathukumalli Lakshmi Nasayana Madhu Mohan[b], and Varadarajan Krishnakumar[c]

[a] Department of Physical Sciences, Bannari Amman Institute of Technology, Sathyamangalam 638401, India
[b] Liquid Crystal Research Laboratory, Bannari Amman Institute of Technology, Sathyamangalam 638401, India
[c] Department of Physics, Periyar University, Salem 636011, India

Reprint requests to V. K.; Fax: 91 427 2345124; E-mail: vkrishna_kumar@yahoo.com

Z. Naturforsch. **64a,** 354 – 360 (2009); received July 2, 2008

A systematic kinetic study of crystallization among two smectogens of higher homologues of the benzylidene aniline series *n*O.*m*, viz. 4O.12 and 8O.12, has been carried out by thermal microscopy, differential scanning calorimetry (DSC), and dielectric studies. The crystallization kinetics was studied by two techniques, viz. the traditional thermal analysis, i. e. DSC, and electrical studies, i. e. capacitance and dielectric loss variation measurements with temperature. The DSC thermograms were run from the crystallization temperature to the isotropic melting temperature for different time intervals. The liquid crystalline behaviour together with the rate of crystallization of smectic ordering in newly synthesized *n*O.*m* compounds were discussed in relation to the kinetophase (which occurs prior to crystallization). The molecular mechanism and dimensionality of crystal growth were computed using the Avrami equation. The characteristic crystallization time (t^*) at each crystallization temperature was deduced from the individual plots of $\log t$ and ΔH. Further, it was observed that the data obtained from DSC and dielectric studies were in good agreement.

Key words: Crystallization Kinetics; Thermal Microscopy; Differential Scanning Calorimetry; Smectic Phases; Dielectric Studies; Kinetophase.

1. Introduction

Liquid crystals exhibit anisotropy like solids as well as fluidity like isotropic liquids and made up of rod-like molecules. These can be obtained by joining two or more phenyl rings or cyclohexyl rings attached with flexible aliphatic end chains to a relatively rigid bridging group and as a function of the temperature [1]. The study of crystallization kinetics [2, 3] is a powerful tool to understand the various mechanisms involved in the crystallization of liquid crystals.

Liquid crystalline materials belonging to the class of benzylidene aniline exhibit a fascinating mesomorphic behaviour associated with distinct molecular ordering; the convenient thermal working range makes them suitable for systematic kinetic investigations. In continuation of our experimental studies [4, 5] on *n*O.*m* and ferroelectric liquid crystals here we present a detailed analysis of two smectogens of higher homologues of the benzylidene aniline series *n*O.*m*, viz. 4O.12 and 8O.12.

2. Experimental

The *n*O.*m* compounds of the present investigation were synthesized and characterized as reported earlier [6]. Their crystallization kinetics, determined by the rate of growth of a particular transition, were performed on a Shimadzu DSC-60 differential scanning calorimeter and an Agilent 4192A LF impedance analyzer. The thermo grams at each crystallization temperature, together with simultaneous phase identification [7] were obtained using an Instec Standalone Temperature Controller (STC 200) supplemented by a Nikon polarizing microscope. The heating and cooling measurements were performed on each member of pure *n*O.*m* compounds (3 – 7 mg sample) using aluminum and/or glass crucibles. A typical differential

scanning calorimetry (DSC) scan for a given sample at each crystallization temperature was as follows. The sample was heated to its isotropic melting temperature with a scan rate of 10 °C min^{-1}; after holding for 1 min to attain thermal equilibrium, the sample was cooled at the same scan rate to its predetermined crystallization temperature. After holding for a requisite time interval at the crystallization temperature, the endothermic peaks were recorded while the sample was cooled to the crystal state also with a scan rate of 10 °C min^{-1}. This process was repeated for each individual member of the *n*O.*m* series at the appropriate preselected crystallization temperatures.

For the elicitation of the dielectric data, the *n*O.*m* sample under investigation was filled in a polyamide buffed cell (Instec Inc.) in its isotropic state with suction. Silver paste and wires were used to connect the electrodes to the cell. The cell was placed in an Instec hot and cold stage (HCS402) equipped with an Instec Standalone Temperature Controller (STC 200). The temperature was monitored and controlled to an accuracy of ± 0.01 °C using a computer. The sample was heated to its isotropic melting temperature with a scan rate of 10 °C min^{-1}; after holding for 1 min to attain thermal equilibrium, the sample was cooled at the same scan rate to its predetermined crystallization temperature. After holding for a requisite time interval at the crystallization temperature, the data of capacitance and dielectric loss was determined for each time interval. This process was repeated for each individual member of the *n*O.*m* series at the appropriate preselected crystallization temperatures.

2.1. Synthesis of the Compounds

The compounds were prepared [6, 7] by condensation of the respective alkoxybenzaldehyde (0.1 mol) and alkyl aniline (0.1 mol) under reflux in absolute ethanol in the presence of a few drops of glacial acetic acid. After refluxing the reactants for 4 h, the solvent was removed by distillation under reduced pressure. The crude sample was subjected to repeated crystallization from cold absolute ethanol, till the transition temperatures were found to be reproducible.

The homologous series of the *N*-(*p*-*n*-alkoxybenzylidene)-*p*-alkylanilines (Schiff's bases) is given by the general molecular formula

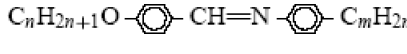

where *n* and *m* represent the number of carbon atoms in the alkoxy and alkyl end chains, respectively. The anilines used for the synthesis of the above compounds are obtained from Sigma Aldrich Chemicals while the alkoxybenzaldehydes were prepared in our laboratory.

Table 1. Transition temperatures (in °C) from thermal microscopy (TM) and differential scanning calorimetry (DSC) of *n*O.*m* compounds. Corresponding enthalpy values (in J/g) are given in parenthesis.

*n*O.*m*	Phase transition	TM	DSC	Dielectric studies (10 kHz)	
				Capacitance	Dielectric loss
8O.12	Iso-SmA	76.1	77.13 (3.27)	75.8	75.9
	SmA-SmB	68.5	68.73 (40.14)	67.7	68.2
	SmB-Crystal	37.1	37.21 (3.54)	37.0	37.0
4O.12	Iso-N	66.1	66.16 (1.47)	66.5	66.6
	N-SmA	53.7	53.99 (*)	53.8	53.7
	SmA-SmB	52.6	52.80 (*)	52.7	52.6
	SmB-Crystal	33.6	33.73 (55.2)	33.5	33.6

* Not well resolved.

2.2. Synthesis of p-n-Butyl/Octyloxybenzaldehyde

To a cyclohexanone solution containing *p*-hydroxybenzaldehyde (1.83 g, 15 mmol) and *n*-butyl bromide (2.7 ml, 20 mmol), 5.15 g *n*-octyl bromide (3.8 ml, 20 mmol) and 5.15 g (37.5 mmol) anhydrous potassium carbonate were slowly added with constant stirring. The reaction mixture was then heated under reflux for 3 h until the evolution of CO_2 ceased. After cooling to room temperature, the reaction mixture was filtered off to remove excess K_2CO_3 and KBr formed during the reaction. The precipitate was washed repeatedly with diethyl ether. Excess ether and cyclohexanone were removed under reduced pressure, and a colourless oil (75% yield) was obtained. The oil was further purified by passing through a silica gel column eluted with a mixture of benzene and acetone in the volume ratio 1 : 4.

3. Result and Discussion

3.1. Phase Identification

The observed phase variants, transition temperatures and corresponding enthalpies obtained by thermal microscopy (TM), dielectric studies and DSC are presented in Table 1. The compounds of the present

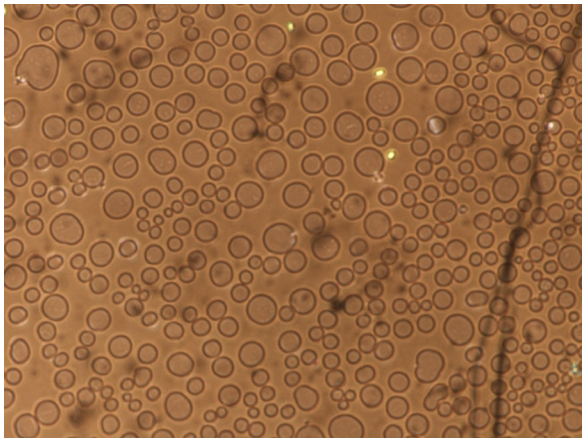

Fig. 1. Nematic phase texture of 4O.12.

*n*O.*m* series are found to exhibit characteristic textures [8], viz. a focal-conic fan texture in the smectic A (SmA) phase, the appearance of transient transition bars across focal-conic fans in the smectic B (SmB) phase. The nematic (N) phase is identified by the figure print texture of nematic droplets (Fig. 1). Further the phase transition temperatures observed by thermal microscopy are found to be in good agreement with those obtained by DSC and dielectric studies.

3.2. Selection of the Thermal Range of Crystallization Temperatures

The procedure for selecting the crystallization temperatures (CT) is described for 4O.12 as a representative member of the present work. The DSC thermo grams of 4O.12 are illustrated in Figure 2. The compound exhibits four distinct transitions in the cooling run at 66.16 °C, 53.99 °C, 52.80 °C, and 33.73 °C manifesting isotropic (Iso) to nematic, nematic to smectic A, smectic A to smectic B, and smectic B to crystal (Cry) transitions. The heat of transition of the isotropic to nematic phase transition is 1.47 J/g while that of the smectic B to crystal phase transition is 55.2 J/g. The transitions from nematic to smectic A and smectic A to smectic B phase are not well resolved in the DSC thermogram. From this data it is inferred that the thermal span of the mesomorphic phase, $(T_{\mathrm{Iso-N}}) - (T_{\mathrm{SmB-Cry}})$, is 33.83 °C. Once the $T_{\mathrm{SmA-SmB}}$ is completed the kinetics of crystallization of the smectic B phase could be investigated over the temperature range between $T_{\mathrm{SmA-SmB}}$ and $T_{\mathrm{SmB-Cry}}$ provided the crystallization kinetics are not too fast.

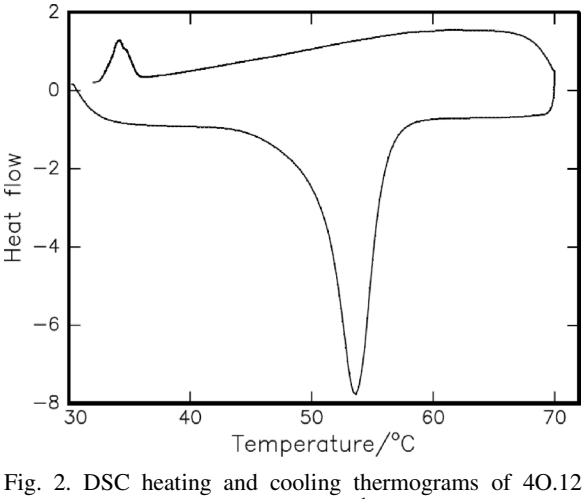

Fig. 2. DSC heating and cooling thermograms of 4O.12 recorded at a scan rate of 10 °C min^{-1}.

3.3. Crystallization Kinetics Determination by DSC

The crystallization kinetics of 4O.12 related to the phase transition from the smectic B phase to the melt is selectively performed at each predetermined crystallization temperature, viz. 44 °C, 45 °C, 46 °C and 47 °C. The sample is held at 44 °C for different time intervals (0.1 to 7 min). The heating curve with a crystallization time of $t = 0$ min is recorded immediately following the quenching of the crystal to melt, at the crystallization temperature of 57 °C. This curve displays only smectic A to isotropic endoderm indicating that the smectic B to smectic A transition has not yet occurred.

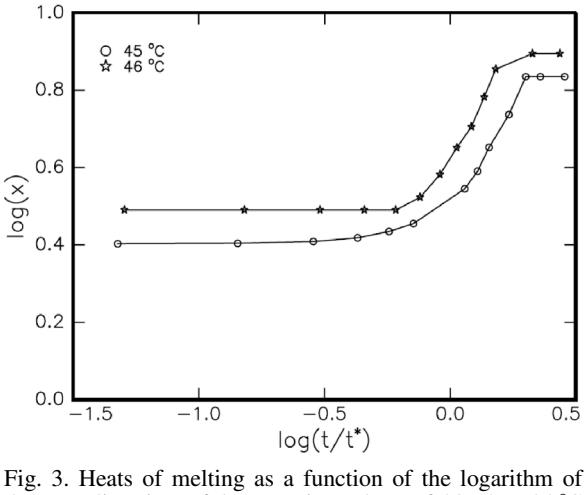

Fig. 3. Heats of melting as a function of the logarithm of the annealing time of the smectic B phase of 4O.12 at 45 °C and 46 °C.

Table 2. Measured crystallization parameters for 63.2% transformation from various smectic mesophases to the crystalline phase of *n*O.*m* compounds experimentally obtained by different techniques.

*n*O.*m*	CT / °C	Thermal studies Differential scanning calorimetry (ΔH)			Electrical studies Dielectric studies (1 kHz) Permittivity (ε')			Dielectric loss (ε'')		
		t^*/s	n	b	t^*/s	n	b	t^*/s	n	b
4O.12	44	42.46	0.501	1.521×10^{-1}	130.91	0.506	0.95×10^{-1}	180.30	0.51	0.707×10^{-1}
	45	158.5	0.845	0.138×10^{-1}	286.15	0.833	0.89×10^{-1}	210.0	0.887	0.869×10^{-1}
	46	68.86	0.960	0.172×10^{-1}	124.62	0.898	0.131×10^{-1}	197.56	0.92	0.81×10^{-1}
	47	125.58	0.325	2.0×10^{-1}	139.0	0.279	2.52×10^{-1}	173.42	0.32	1.89×10^{-1}
8O.12	57	23.35	0.105	0.066×10^{-1}	161.69	0.378	1.462×10^{-1}	176.92	0.374	1.44×10^{-1}
	58	39.81	0.632	0.974×10^{-1}	213.79	0.342	1.59×10^{-1}	462.7	0.362	1.05×10^{-1}
	59	42.41	0.820	4.850×10^{-1}	98.22	0.260	3.03×10^{-1}	213.21	0.258	2.507×10^{-1}
	60	15.84	0.160	0.534×10^{-1}	134.89	0.107	5.73×10^{-1}	171.71	0.171	4.148×10^{-1}
	62	35.14	0.176	0.56×10^{-1}	137.08	0.301	2.27×10^{-1}	109.39	0.404	1.50×10^{-1}

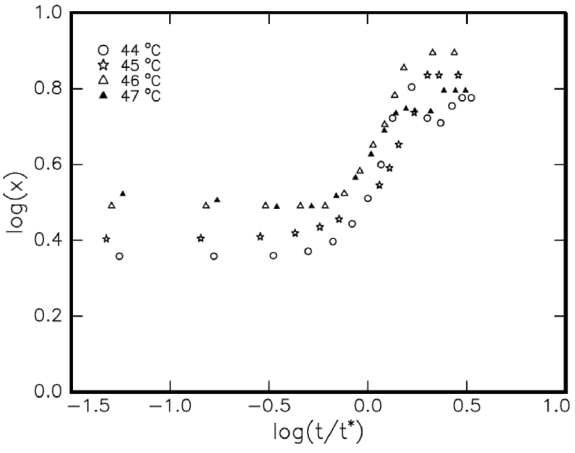

Fig. 4. Heats of melting of the mesomorphic phase of 4O.12 versus the logarithm of the annealing time for different temperatures, obtained by shifting data along the log$t$ axis to 44 °C.

The enthalpies of individual transitions at different time intervals are calculated at each crystallization temperature, and the corresponding data are plotted against the corresponding logarithm of time intervals for each member of the n.Om series. Figure 3 shows plots for the crystallization of 4O.12 at 45 °C and 46 °C. These plots have an identical shape, apart from the shift in the log$t$ axis suggesting limitations of the rate of crystallization kinetics [9].

Plots of the heats of melting of the mesomorphic phase, viz. the logarithm of the annealing time for different crystallization temperatures of 4O.12, obtained by shifting data along the log$t$ axis to the 44 °C curve are depicted in Figure 4. Such master curves strongly suggest that the same mechanism is valid for crystallization of both the smectic A and smectic B phases. As expected [9], the overall nucleation rate depends on the formation of the liquid crystalline phase, but the growth rate is independent of the formation of the liquid crystalline phase.

Similar experimental studies are carried out for the measurement of crystallization kinetics of the other compound (8O.12). The corresponding data of crystallization time t^* along with the calculated crystal growth parameters for different crystallization temperatures are summarized in Table 2, which includes all results relevant to the following sections.

3.4. Dielectric Studies

Dielectric studies enable to identify the phase transition temperatures and the thermal range of individual phases. This study is a sophisticated tool to detect the second-order transitions which can not be identified by DSC studies.

To calculate the lead capacitance the liquid crystal cell is calibrated with a known substance (benzene). Further, the empty liquid crystal cell is also calibrated in the range temperature of 25 °C to 150 °C and in the range frequency of 100 Hz to 1 MHz, respectively. The compounds 4O.12 and 8O.12, in their isotropic state, are filled in 4-micron spacer polyamide buffed cells with suction, the silver leads are pulled of to excite the cell with a frequency of 10 kHz, obtained from an Agilent low-frequency impedance analyzer (4192A). The liquid crystal cell with the compounds is heated to its isotropic state and held for 10 min to attain thermal equilibrium. Then it is cooled until crystallazation at a programmed scan rate of 0.1 °C/min with an accuracy of ±0.01 °C. The liquid crystal cell is placed in an Instec hot stage and is observed under crossed polars of a Nikon polarizing microscope. Simultaneous obser-

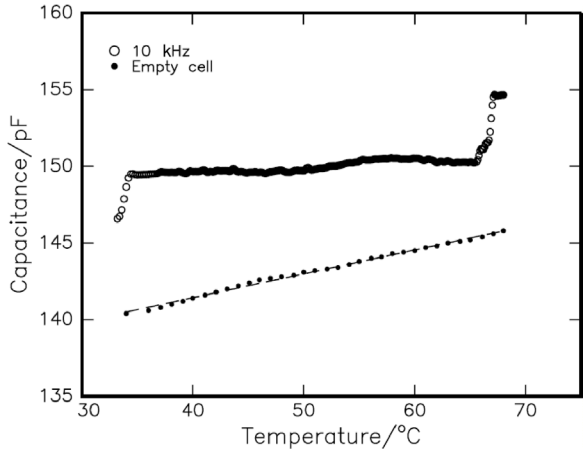

Fig. 5. Temperature variation of the capacitance of 4O.12 at 10 kHz. The solid line indicates the temperature variation of the empty cell capacitance.

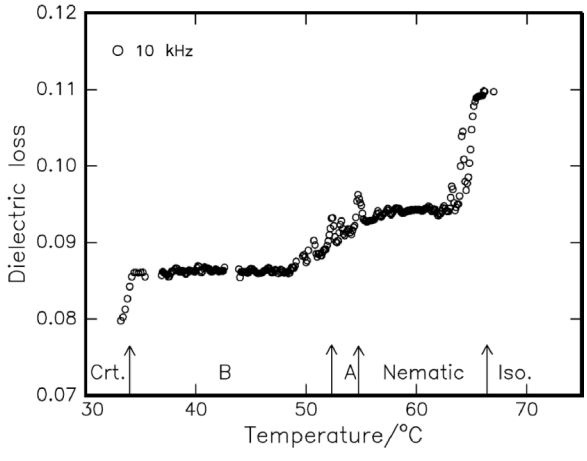

Fig. 6. Temperature variation of the dielectric loss at 10 kHz identifying various liquid crystalline phases of 4O.12.

vation of the liquid crystal texture through the polarizing microscope along with the dielectric data confirms the formation and identification of the various smectic phases.

Compound 4O.12 is chosen as a representative member of the present work and the plot of its capacitance versus temperature at 10 kHz is depicted in Figure 5. The variation of the capacitance with the temperature of the empty cell is also shown in Fig. 5 as a solid line. The corresponding dielectric loss is illustrated in Figure 6. The transition temperatures obtained by DSC, polarizing microscopic studies and dielectric studies are compared in Table 1. The following points are noted from the dielectric studies:

a) At isotropic to nematic transition, a sudden variation in both the profiles at 66.5 °C and 66.6 °C is observed, indicating the formation of the nematic phase. This transition occurs at 66.1 °C according to polarizing microscopic textural observations, which concur with the dielectric studies.

b) The unaltered variation of the magnitudes of the capacitance and dielectric loss with lowering the temperature in the thermal range 66.5 °C to 53.7 °C is attributed to the stabilization of the smectic A phase.

c) An anomaly in the capacitance and dielectric loss spectrum in the form of a peak at 52.6 °C is attributed to the transition from the smectic A phase to the smectic B phase.

d) The crystallization at 33.6 °C is evidenced by a sudden fall in the magnitudes of capacitance and dielectric loss data as can been seen in Figs. 5 and 6, respectively.

It is prudent to mention that in the present homologous series the experimental results of 4O.12 follow the same trend of 8O.12 dielectric studies, as expected. These results are tabulated in Table 1. Furthermore, the transition temperatures obtained by various techniques, namely dielectric studies, polarizing microscopic textural observations and differential scanning calorimetric thermograms, are concurring with each other as can be seen from Table 1.

3.5. Crystallization Kinetics Determination by Dielectric Studies

It was earlier proposed by us [5] that the crystallization kinetics can also be studied and analyzed at a selected frequency using dielectric data. The crystallization kinetics of 8O.12 relating to the phase transition from the smectic B phase to the melt is selectively performed at each predetermined crystallization temperature, viz. 57 °C, 58 °C, 59 °C, 60 °C, and 62 °C at an excitation frequency of 1 kHz. The sample is held at 57 °C for different time intervals (0.1 to 10 min). The dielectric data (capacitance and dielectric loss) at 1 kHz excitation frequency with a crystallization time of $t = 0$ to 10 min are recorded immediately following the quenching of the crystal to melt, at the crystallization temperature 57 °C. The capacitance and dielectric loss values for individual transitions at different time intervals are noted at each crystallization temperature, and the corresponding data are plotted against the corresponding logarithm of time intervals for each member of the n.Om series. Crystallization of 4O.12

obtained by this technique at 45 °C and 46 °C is identical to that of DSC data curves suggesting the existence of the same mechanism in the rate of crystallization kinetics [4].

3.6. The Process of Crystallization

In general, the kinetics of crystallization involving the rate of growth of small domains in a smectic phase is manifested equally by its temperature and time. Temperature dependence of nucleation, taking place as a homogenous process over a constant period of time, leads to the phenomenon of sporadic growth. In addition, defects and impurities in the compound have a pronounce influence on the nucleation process [9]. Further contributions from solid state transformations, where growth occurs only at the surface of the nuclei, hamper the overall rate of phase transformation and the dimensional geometry of the rowing domains.

It is well known that the crystallization process involving the fraction of the transformed volume x, at a time t measured since the beginning of the crystallization process, is described by the Avrami equation [2, 3]

$$x = 1 - \exp(-bt^n), \tag{1}$$

where the constants b and n depend on the nucleation mechanism and the dimensionality of the growing domains, respectively. The transformed volume x at a crystallization time t is given by $\Delta H/\Delta H_o$, where ΔH is the crystal heat of melt measured at the time t and ΔH_o is the maximum value obtained from the plateau of the individual master curves (Fig. 4). The similar argument holds good for the dielectric data $\Delta\varepsilon'/\Delta\varepsilon'_o$ and $\Delta\varepsilon'/\Delta\varepsilon''_o$, where $\Delta\varepsilon'$ and $\Delta\varepsilon''$ are the values of capacitance and dielectric loss at the time t and $\Delta\varepsilon'$ and $\Delta\varepsilon''_o$ are the maximum values obtained from the plateau of the individual master curves.

If the kinetics of crystallization from the corresponding smectic phases are described by (1), the data for all the crystallization temperatures can be applied in the single equation [9]

$$x = 1 - \exp[1 - (t/t^*)^n], \tag{2}$$

where $t^* = b^{-1/n}$. Further, the characteristic time t^* can be experimentally determined since, at $t = t^*$, $x = 0.632$. Substituting the values of t^* and x in (1), the constants b and n are obtained at a specific crystallization temperature. It is found from the experimental data that the constant n, which manifests the dimensionality of the growing domains, is almost unaltered while the magnitude of the constant b, which governs the nucleation mechanism, varies in the order of 10^{-1} for the compounds studied. The data of the constants n and b experimentally obtained by DSC and dielectric studies (capacitance and dielectric loss) for various specific crystallization temperatures of 4O.12 and 8O.12 are tabulated in Table 2.

For a specific crystallization temperature, the values of constants n and b are found to be unaltered in both thermal and electrical studies implying that the same type of nucleation mechanism is taking place in both the *n*O.*m* compounds. The trend of the magnitude of the two constants n and b is found to be in agreement with the data reported for discotic [9] and smectic [4] mesophases. The variation of the magnitude of n in both the *n*O.*m* compounds is attributed to the sporadic nucleation and growth in two dimensions.

3.7. Influence of the Orthogonal Smectic B Phase Variant on Crystallization Kinetics

The phase sequence in liquid crystals has a pronounced influence on their crystallization kinetics. The kineto phase, which occurs prior to crystallization, is solely responsible for many combinational factors of the crystallization mechanism.

In the present study of 4O.12 and 8O.12 compounds the kineto phase prior to crystallization is the smectic B phase. Our previous studies [4] on different *n*O.*m* compounds exhibiting various kineto phases concur with data of the present investigations. Further in the smectic B phase, as expected, the rate of crystallization is rapid as it is close to the crystalline phase. It is a known fact that crystallization kinetics are fast for crystallization temperatures (CT) near to the crystalline phase, and slow when the CT is near the isotropic melt.

3.8. Influence of Alkyloxy Carbon Atoms

Both the 4O.12 and 8O.12 compounds have the same kinetic phase, viz. smectic B. The data from Table 1 suggest that the liquid-crystalline phase transition temperature is 34 °C and 29 °C for 4O.12 and 8O.12, respectively. Further the kinetoc phase (smectic B) thermal stability range is decreased from 30 °C to 20 °C in both compounds with increasing alkyoxy carbon atom number, however, as expected, the isotropic clearing point shifts to higher temperature

with increase in the carbon atom chain length. It is evident that the degree of variation of the dimensionality parameter n infers a unique crystallization mechanism for these compounds. A possible explanation for the crystallization dimensionality is a sporadic nucleation and growth involving a homogenous process of continuous nucleation over a constant time [9]. Furthermore the volume transformation calculated at individual a time t^* is in accordance with (2) which strongly implies the completion of the crystallization process.

4. Conclusions

1. In orthogonal ordering (smectic B phase) the formation of an ordered domain occurs which converts to a stable nucleus that initiates the aggregation of the surrounding molecules to form layered domains. The origin of this nucleus is critical since its formation proceeds until it reaches a sufficient size to initiate the crystallization process.

2. We propose that this process of crystallization is controlled by either lamellar or inter-layer distances in a non-tilted (smectic B phase) kineto phase. In such a process of seed nucleation, factors relating to the smectic layer play an important role. A particular molecule in the lower smectic layer first acquires the requisite energy to allow the formation of ordered domains, which in turn propagate crystallization to the adjacent smectic layers. These ordered domains will further proceed through the smectic layers by a process of successive addition of molecules from neighbouring layers leading to sporadic nucleation and growth in two dimensions. This process continues until the crystallization is completed.

Acknowledgements

The authors thank the Management of Bannari Amman Institute of Technology Sathyamangalam, India, for providing the laboratory and other infrastructural facilities. M.L.N.M. M acknowledges financial support provided by Department of Science and Technology, New Delhi, India, All India Council of Technical Education, New Delhi, India, and Defence Research Development Organization, New Delhi, India.

[1] D. Demus, Liquid Crystals: Phase Types Structures and Chemistry of Liquid Crystals, Springer, New York 1994.
[2] M. Avrami, J. Chem. Phys. **7**, 1103 (1939).
[3] M. Avrami, J. Chem. Phys. **8**, 212 (1940).
[4] M. L. N. Madhu Mohan, B. Arunachalam, and C. R. Aravind Sankar, Met. Mat. Trans. A **39**, 1192 (2008); M. L. N. Madhu Mohan and B. Arunachalam, Z. Naturforsch. **63a**, 435 (2008); T. Chitravel, M. L. N. Madhu Mohan, and V. Krishnakumar, Mol. Cryst. Liq. Cryst. **493**, 17 (2008); P. A. Kumar, M. L. N. Madhu Mohan, and V. G. K. M. Pisipati, Liq. Cryst. **27**, 727 (2000).
[5] M. L. N. Madhu Mohan, Romanian J. Phys., submitted.
[6] V. G. K. M. Pisipati, N. V. S. Rao, G. P. Rani, and P. Bhaskara Rao, Mol. Cryst. Liq. Cryst. **210**, 165 (1991).
[7] P. Kelker and B. Scheurle, Angew Chem. Int. Ed. Engl. **8**, 884 (1969).
[8] G. W. Gray and J. W.Goodby, Smectic Liquid Crystals – Textures and Structures, Leonard Hill, Glasgow 1984.
[9] Z. R. He, Y. Zhao, and A. Caille, Liq. Cryst. **23**, 317 (1997).